JST&M 1(2021), 20 – 29
DOI: 10.57131/jstm.2021.1.3

Original scientific paper

PROPERTIES OF AUSTENITE STAINLESS STEEL MICROALLOYED WITH TELLURIUM AND ZIRCONIUM

Derviš Mujagić[1], Aida Imamović[2] and Mustafa Hadžalić[3]

[1]University of Zenica, Institute "Kemal Kapetanović";
[2]The University of Zenica, Faculty of Metallurgy and Technology;
[3] University of Zenica, Institute "Kemal Kapetanović";

ABSTRACT

Stainless steel X8CrNiS18-9 (standard EN 10088-3: 2005) is the most commonly used austenitic stainless steel due to its good machinability. This steel has high mechanical and working properties thanks to a complex alloying, primarily with the elements such as chromium and nickel. The content of sulphur present in the steel from 0.15 to 0.35% improves machinability. Microalloying with tellurium and zirconium (individually and in combination) in most cases leads to improved properties of this stainless steel, compared to melt without alloying additives, e.g. the melt microalloyed with tellurium and especially melt microalloyed with zirconium and tellurium has significantly better machinability compared to the melt without alloying elements

The addition of sulphur, which is the cheapest available additive for free machining, will impair not only the transverse strength and toughness but also the corrosion resistance. However, while sulphur improves machinability at the same time decreases the mechanical properties particularly toughness.

This work aims to test machinability, corrosion resistance, and mechanical properties of the mentioned steel, as well as the chemical composition of non-metallic inclusions.

Keywords: nonmetallic inclusions; tellurium; zirconium; machinability; corrosion resistance; mechanical properties.

Corresponding Author:
Derviš Mujagić,
University of Zenica, Institute "Kemal Kapetanović"
Travnička cesta 7, 72000 Zenica, B&H
Tel.: +387 61 588 883; fax: +387 32 247 980.
E-mail address: dervis.mujagic@unze.ba; dervismujagic@yahoo.com

1. INTRODUCTION

Stainless steel X8CrNiS18-9 is austenitic stainless steel for free cutting on automated machine tools. One of the key design requirements is the highest material removal per unit time and chip breakability. Therefore, this steel contains an increased sulphur content to obtain a larger amount of manganese sulfide. In addition to the amount of manganese sulphides, their shape and way of distribution in the steel matrix are also very important for the mechanical properties of steel as well as corrosion resistance. The shape, size, and distribution of manganese sulphides can be influenced by the addition of elements having a high oxygen affinity such as titanium, magnesium, or zirconium, by the addition of calcium or REM elements, or by the addition of tellurium.

In this paper, the focus is on the action of zirconium and tellurium, both individually and in combination with the form and chemical composition of manganese sulphides.

The addition of tellurium to improve the cut surface is due to the lubrication ability of manganese telluride. Tellurium occurs in

steels in inclusions in the form of manganese (sulpho) telluride ($MnTe_xS_{(1-x)}$), or as a white envelope of manganese sulphide, or in the form of globular inclusions, which are at the base of manganese sulphide or manganese silicate [1].

Manganese telluride (MnTe) inclusions and is more effective than sulphur for machinability of austenitic stainless steels. As well as selenium, it also promotes globularization and expansion of sulphide inclusions. Although tellurium is now recognized as a powerful sulphur modifier as well as a machinability additive when used in combination with lead and sulphur [2], it also has a downside because it causes problems with hot processing of austenitic stainless steels and has not been used for commercial purposes [3].

The function of zirconium is not to remain in melt steel, but to remove impurities of oxygen, sulphur, and nitrogen, or modify inclusions by forming complex sulphides and oxy-sulphides. Zirconium sulphide is significantly more stable than manganese sulphide in steel. Therefore, if sufficient free zirconium is available during the early stages of solidification of liquid steel, zirconium sulphide will be formed and prevent the formation of manganese sulphide. Zirconium sulphide is much more refractory than manganese sulphide and is virtually undeformable during hot rolling [4].

The literature suggests that the optimal combination of higher sulphur content to improve machinability and zirconium for better impact characteristics provides the steel with acceptable machinability and ductility criteria [5]. It has been observed that even a small amount of zirconium causes clusters of sulphide, nitride, and oxide inclusions in cast steel; this could indicate the effect of ZrO_2 on nucleus formation for the rest of the inclusions [6].

2. EXPERIMENTAL RESEARCH AND TEST RESULTS

The research aimed to examine machinability, corrosion resistance, and mechanical properties of austenitic stainless steel X8CrNiS18-9 without and with the addition of zirconium and tellurium. Production of austenitic stainless steel X8CrNiS18-9 was performed in a vacuum induction furnace at the Institute "Kemal Kapetanović" in Zenica. Four melt variants were made, the weight of the ingot is about 7 kg, Table 1. The first is without alloying elements, the second is alloyed with zirconium, the third with tellurium, and finally the fourth with both elements, zirconium, and tellurium. The ingots were processed by forging (approx. □50 mm), hot rolling (the final dimensions of the rectangular cross-section are 14 x 50 mm), and heat treatment. Chemical analysis of the four melt variants is given in Table 1. SEM Elemental Mapping and EDS scan methods were used to examine the exact chemical composition of sulphides in masse percent.

Table 1. Chemical analysis of melt variants [7]

Melt variants	Chemical composition (%)								
	C	Si	Mn	P	S	Cr	Ni	Zr	Te
Without alloying elements	0.03	0.42	0.61	0.021	0.18	18.3	9.4	–	–
Alloyed with Zr	0.04	0.35	0.75	0.021	0.17	18.8	9.4	0.016	–
Alloyed with Te	0.05	0.40	0.80	0.010	0.16	18.9	9.3	–	0.033
Alloyed with Zr and Te	0.03	0.47	0.72	0.012	0.18	18.5	8.9	0.007	0.040

2.1. Machinability

In the Laboratory for metal cutting and machine tools of the Faculty of Mechanical Engineering in Zenica, the machinability test of the semifabricate after forging was done, based on the estimation of parameters of the cutting force. Testing on all samples was performed under the same treatment regime. The results of the cutting force tests

(individual forces F_x, F_y, and F_z as well as the resultant force F_R) are given in Table 2.
The melt microalloyed with zirconium has about 3% worse machinability compared to melt without alloying elements. However melt microalloyed with tellurium has up to 12% better machinability, while especially melt microalloyed with zirconium and tellurium even up to 22% better machinability compared to the melt without alloying elements.

Table 2. The results of the cutting force tests [7]

Melt variants	Cutting force (N)			The resultant force F_R (N)
	Component F_x	Component F_y	Component F_z	
Without alloying elements	180	218	361	458,52
Alloyed with Zr	193	235	362	472,77
Alloyed with Te	154	200	317	405,22
Alloyed with Zr and Te	137	164	289	359,42

2.2. Corrosion resistance

General corrosion tests for X8CrNiS18-9 stainless steel samples were performed on a potentiostat/galvanostat PAR 263A-2 device in an electrochemical cell prescribed by ASTM G5-94. The samples were tested in a solution of 1% HCl at room temperature. The solution was previously deaerated with argon for 30 minutes as provided by ASTM G5-94. To test the general corrosion of the X8CrNiS18-9 stainless steel samples, the Tafel Directional Extrapolation Method described by ASTM G3-89 was used. The results of testing the general corrosion rate of these samples are given in Table 3.

About the effect of zirconium and tellurium microalloying on the corrosion rate of austenitic stainless steel X8CrNiS18-9, it can be concluded that melt alloyed with tellurium shows a marked increase in corrosion rate compared to the melt without alloying additives. However, the melt which is microalloyed with the zirconium and tellurium shows a significant reduction in corrosion rate compared to melt without alloying additives, while melt microalloyed only with zirconium shows a further reduction of corrosion rate compared to melt microalloyed with the zirconium and tellurium.

Table 3. Test results for general corrosion rate [7]

Melt variants	Corrosion current, I_{Corr} (μA)	Corrosion rate, v_{Corr} (mm/year)	Open Circuit Potential, $E_{(I=0)}$ (mV)
Without alloying elements	4.266	4.955	-475.320
Alloyed with Zr	3.175	3.687	-474.438
Alloyed with Te	8.949	10.390	-504.517
Alloyed with Zr and Te	3.523	4.092	-472.957

2.3. Mechanical properties

After the rolling process was completed, specimens were prepared for mechanical testing (tensile properties and impact toughness testing). The tests were performed at the Mechanical Laboratory of the Institute "Kemal Kapetanović" in Zenica. The results of the tensile properties and impact toughness testing are given in Table 4.
The impact toughness value is even slightly higher for all three melt (microalloyed with zirconium, tellurium, and zirconium and tellurium) compared to the melt without alloying elements, and the highest value of impact toughness has the melt microalloyed with zirconium and tellurium.

2.4. Testing of samples at SEM in a rolled condition

The tests were performed at the Scanning Electron Microscope (SEM) type JEOL JSM

5610 of Japanese production at the Faculty of Natural Sciences and Engineering, University of Ljubljana. The microscope works with excitation energy up to 30 keV. The theoretical increase is up to 300000x. The microscope also has an EDS detector. It can do semi-quantitative and qualitative analyzes. Tests were carried out on samples in a rolled condition as the final stage of processing. Point analysis and mapping were done for each of these samples.

Figure 1 gives a mapping showing the inclusions of the sample without the addition of alloying elements. It is clear from the picture that the inclusions from the SEM image (Figure 1a) are almost identical to those in the images showing the position of manganese and sulphur (Figures 1b and 1c).

Table 4. Test results of tensile properties and impact toughness in rolled condition [7]

Melt variants	Conventional yield strength $R_{p0,2}$ (N/mm²)	Tensile strength R_m(N/mm²)	Elongation A (%)	Reduction Z (%)	Impact toughness (J) KV 300 J	
					Individually	Average
Without alloying elements	349	670	50,0	70	60; 56; 56	57
Alloyed with Zr	321	653	51,5	63	55; 69; 55	60
Alloyed with Te	314	635	46,5	59	58; 69; 60	62
Alloyed with Zr and Te	312	629	47,5	53	64; 69; 62	65
Standard EN 10088-3 Stainless steel	min. 190	500 – 750	min. 35,0	–	–	–

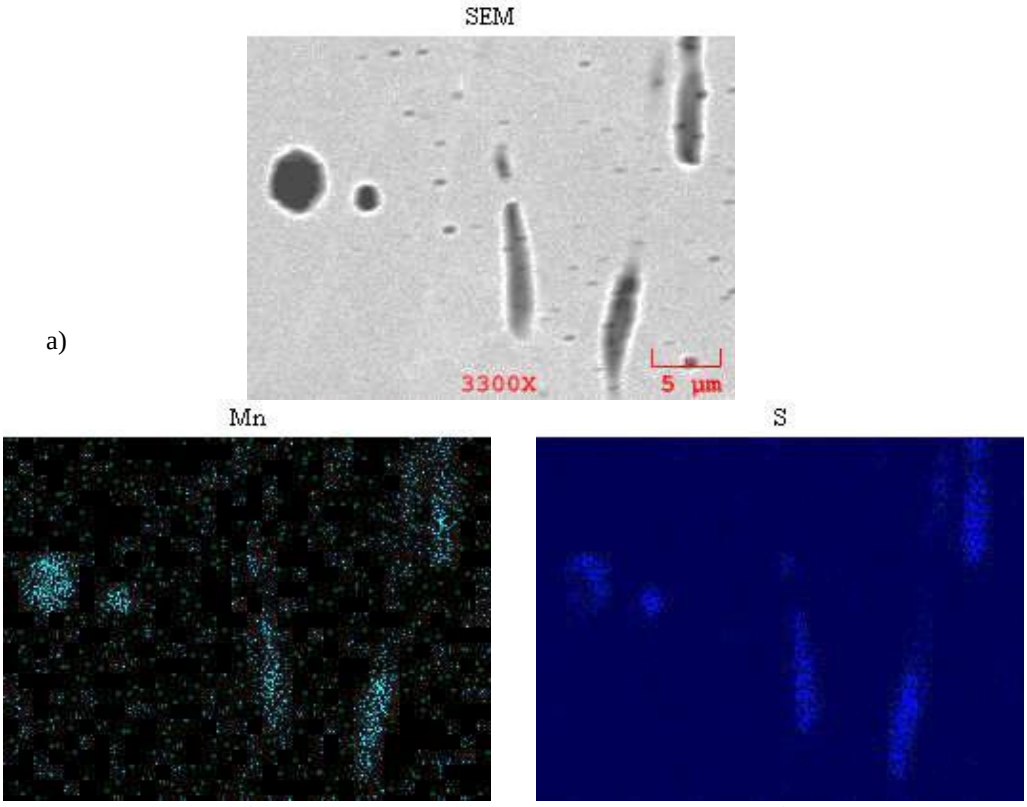

a) b) c)

Figure 1. Mapping of the sample without additions of alloying elements:
a) SEM image; b) and c) elements Mn and S [7]

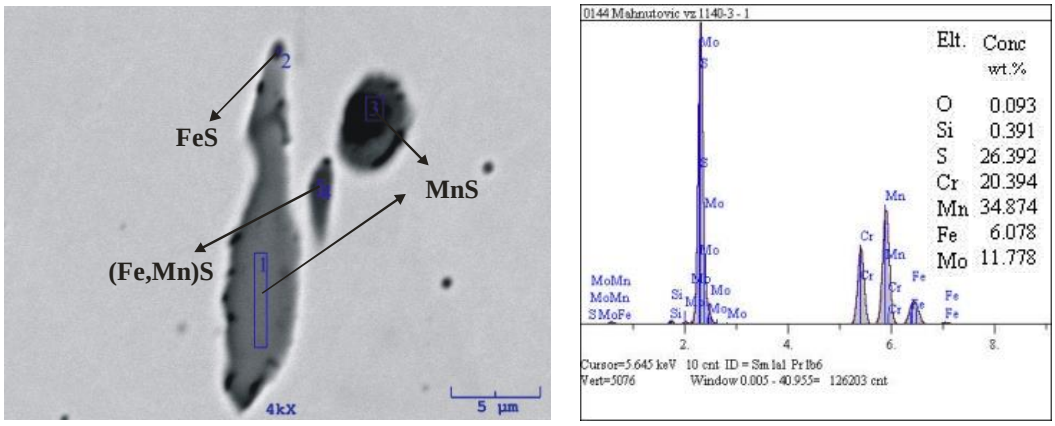

a) b)

Figure 2. Spot analysis of sample inclusions without alloying elements: a) SEM image; b) diagram of detected elements with chemical analysis in mass percentages [7]

Figure 2 shows the spotted analysis of sample inclusions without alloying elements. Based on the analysis of the below diagram, it can be concluded that the inclusions formed in the sample are mainly the inclusion of manganese sulphides (point 1 in SEM, diagram 2b).

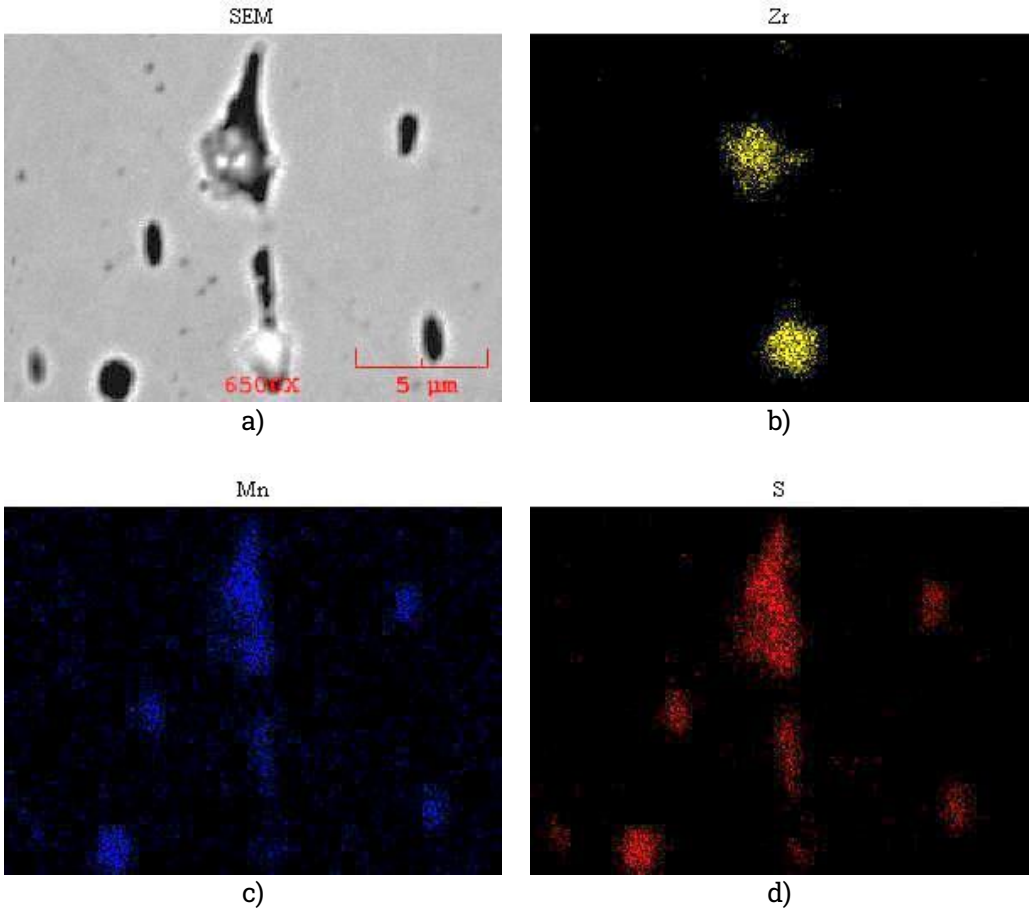

a) b)

c) d)

Figure 3. Mapping a sample with the addition of zirconium: a) SEM image; b) - d) Zr, Mn, and S elements [7]

Figure 3 is shown a mapping of the inclusions of the sample with the addition of zirconium. It is clear from the picture that the inclusions from the SEM image (Figure 3a) are almost identical to those in the images showing the position of the

manganese and sulphur (Figures 3c and 3d). Also, based on the comparison of the SEM image with an image indicating the zirconium distribution, it can be concluded that the zirconium is at its maximum in two different locations within the two different inclusion (Figure 3b).

Figure 4 shows the spotted analysis of individual inclusions of the sample with the addition of zirconium. Based on the analysis of the below diagrams, it can be concluded that the shown inclusion is a complex inclusion, which, in addition to manganese sulphide, contains other elements, in this case, zirconium and oxygen (point 1 and diagram 4b), which are probably formed in part by zirconium oxide. The tendency of zirconium to form inclusions (Zr, Mn)S in zirconium steels, which have a similar color and morphology to that of manganese sulphide, can be observed by looking at point 4 in the SEM figure and diagram 4c, which is also confirmed in the reference [8].

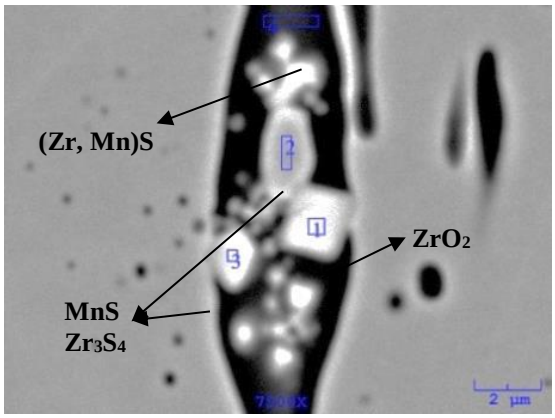

a)

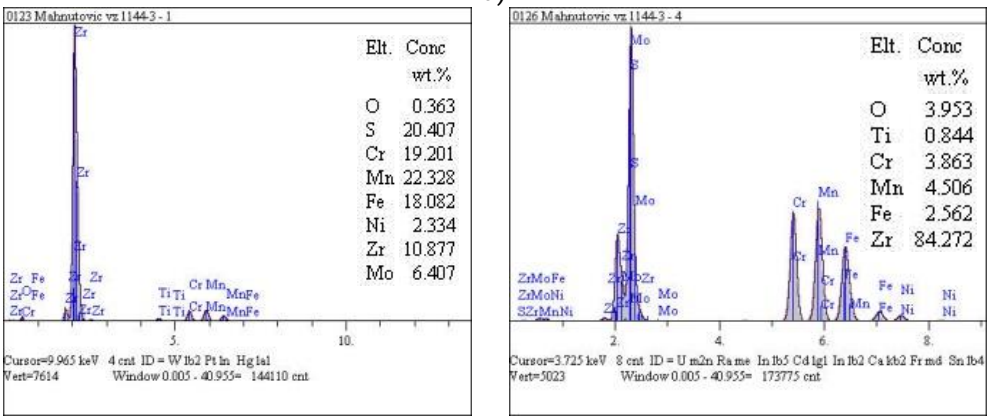

b) c)

Figure 4. Spot analysis of the inclusion of the sample with the addition of zirconium: a) SEM image; b) and c) diagrams of detected elements with chemical analysis in mass percentages [7]

Figure 5 shows mapping the inclusions of the sample with the addition of tellurium. It is clear from the picture that the inclusions from the SEM image (Figure 5a) are almost identical to those in the images showing the position of manganese and sulphur (Figures 5c and 5d). Also, based on the comparison of the SEM image with the image indicating the tellurium distribution, it can be concluded that the tellurium is practically in all the inclusions shown in the SEM picture, mainly at their ends (Figure 5b).

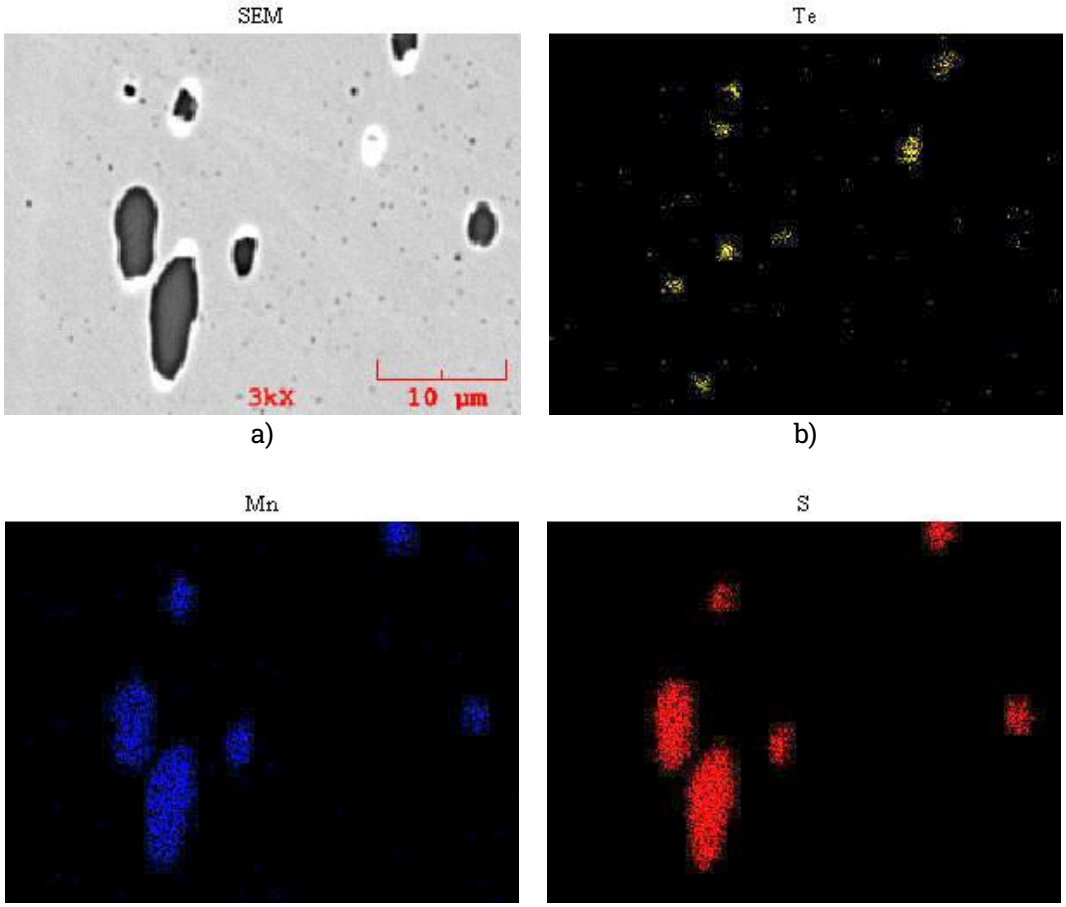

Figure 5. Mapping a sample with the addition of tellurium: a) SEM image; b) - d) Te, Mn, and S elements [7]

Figure 6 shows a spot analysis of the inclusions of the sample with the addition of tellurium. Based on the content of individual elements in the below diagrams, it can be concluded that the displayed larger inclusion is complex inclusion, which, in addition to manganese sulphide (point 2), contains other elements, in this case, tellurium (point 1, diagram 6b, as well as edge sections of the inclusions).

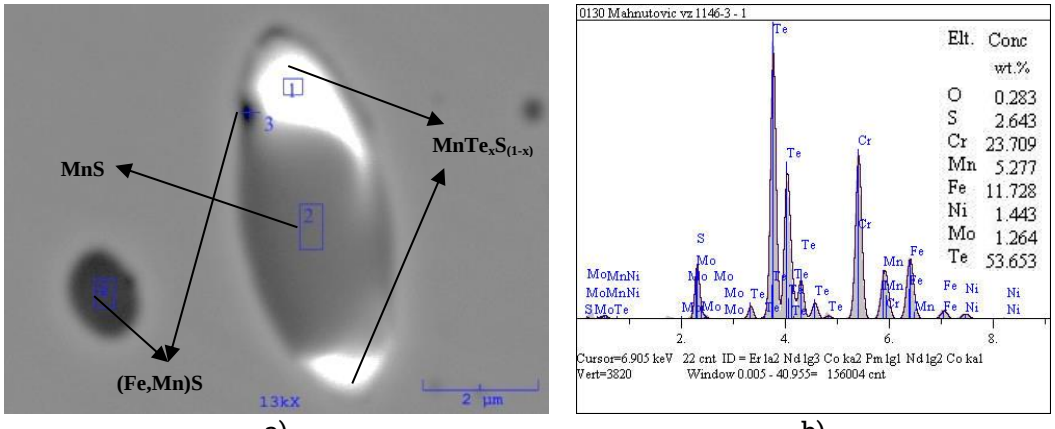

Figure 6. Spot analysis of the inclusion of the sample with the addition of tellurium: a) SEM image; b) diagram of detected elements with chemical analysis in mass percentages [7]

Figure 7 shows a mapping where each of the elements represented by the mapping is in relation to the SEM image (Figure 7a), which shows the inclusions of the sample with the addition of zirconium and tellurium.

On the basis of the image can be concluded that the positions of the manganese and sulphur virtually overlap (Figures 7b and 7c), which tells us that the displayed inclusion is basically the inclusion of manganese sulphide. Also, by comparing the SEM image with images showing the positions of zirconium and tellurium, it can be concluded that zirconium is largely the basis of the inclusions, at least in its central part (Figure 7d), while the tellurium is mostly located on the edge of inclusion (Figure 7e).

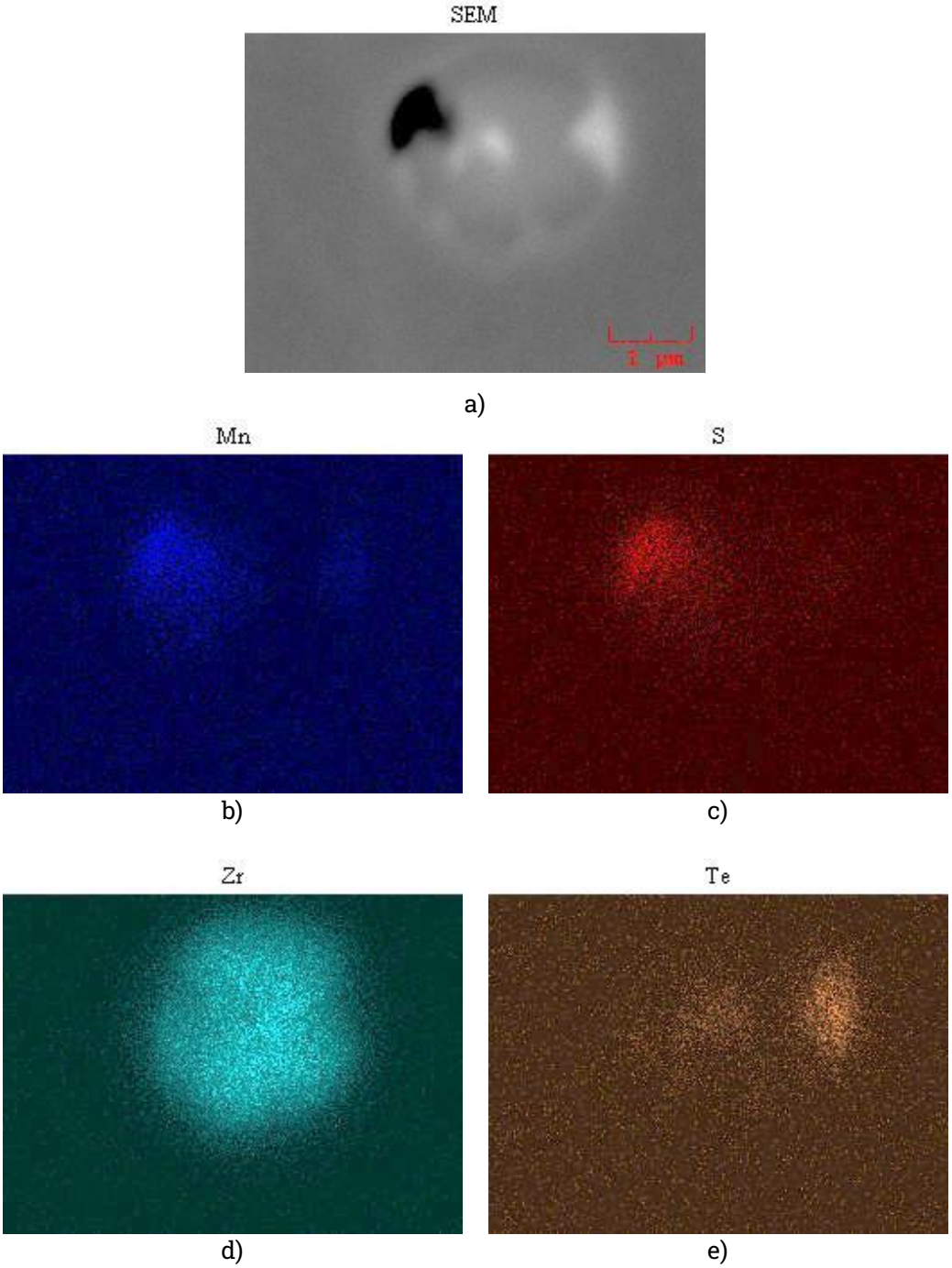

Figure 7. Mapping a sample with the addition of zirconium and tellurium: a) SEM image; b) - e) Mn, S, Fe, Zr and Te elements [7]

Figure 8 shows a spot analysis of the inclusions of the sample with the addition of zirconium and tellurium. Based on the content of individual elements in the below diagrams, it can be concluded that the displayed larger inclusion is complex inclusion, which, in addition to manganese sulphide (point 3), contains other elements, in this case, tellurium (point 1, diagram 9b, as well as edge sections of the inclusion), and zirconium (point 2, diagram 8c, as well as central sections of the inclusion). The tendency of zirconium to form inclusions (Zr, Mn)S, which have a similar color and morphology to that of manganese sulphide, can be observed by looking at point 1 in the SEM figure and diagram 8b.

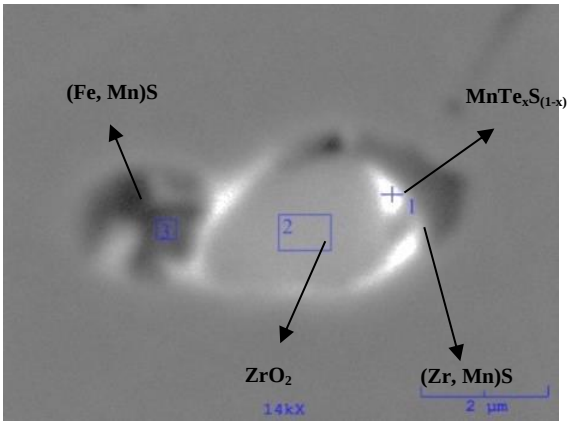

a)

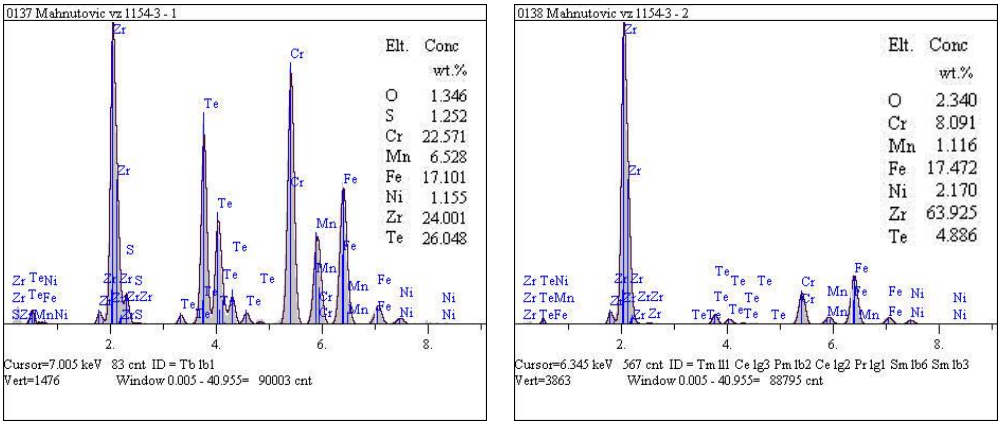

b) c)

Figure 8. Spot analysis of inclusion of the sample with addition of Zr and Te: a) SEM image; b) and c) diagrams of detected elements with chemical analysis in mass percentages [7]

3. CONCLUSIONS

After all the tests performed, it is possible to draw the following conclusions:

- The melt microalloyed with zirconium has slightly worse machinability, but melt microalloyed with tellurium and especially melt microalloyed with zirconium and tellurium has significantly better machinability compared to the melt without alloying elements.
- The melt microalloyed with tellurium has a significantly worse corrosion rate, but melt microalloyed with zirconium and tellurium and especially melt microalloyed with zirconium has significantly better corrosion rate compared to the melt without alloying elements.
- All values of tensile properties (tensile strength, conventional yield strength, elongation, and reduction) are within the limits prescribed by the relevant standard for the material specified.
- The basic types of inclusions in this steel are manganese sulphides. They

can be modified by the addition of zirconium and tellurium, and on one side they will provide good machinability and, on the other hand, will not adversely affect the properties of austenitic stainless steel X8CrNiS18-9.

Conflicts of Interest:
The authors declare no conflict of interest.

References:

[1] K. Hribar, *Vpliv kovinskih in nekovinskih dodatkov na obliko vključkov in tehnološke lastnosti jekel* [Magistrsko delo], FNT, Univerza v Ljubljani, 1981.

[2] J. Grum, Quantitative analysis of sulphide inclusions in free-cutting steels and their influence on machinability, *Acta Stereologica*, 18 (1999), p. 319-331

[3] D. Mujagić, A. Imamović, M. Oruč, S. Muhamedagić, Analysis of the type and chemical content of the inclusion on SEM of the stainless steel with and without the addition of Zr and Te, In: 4th International Conference „NEW TECHNOLOGIES NT-2018" Development and Application, Sarajevo, 14-16 June 2018, p. 72-79.

[4] M. Taguchi, H. Sumitomo, R. Ishibashi, Y. Aono, Effect of Zirconium Oxide Addition on Mechanical Properties in Ultrafine Grained Ferritic Stainless Steels, *Materials Transactions*, 49 (2008), p. 1303 - 1310

[5] D. Bhattacharya, Effect of Sulfur and Zirconium on the Machinability and Mechanical Properties of AISI 1045 Steels, *Metallurgical Transactions A*, 12 (1981), p. 973-985

[6] http://www.imim.pl/files/archiwum/Vol1_2015/12.pdf (january 2020)

[7] D. Mujagić, *Doprinos istraživanju uticaja mikrolegiranja sa borom, cirkonijem i telurom na osobine austeninog nehrđajućeg čelika sa dodatkom sumpora X8CrNiS18-9* [Doktorska disertacija], MTF, Univerzitet u Zenici, Zenica, 2017.

[8] https://pure.strath.ac.uk/portal/files/39731393/Baker et al Mats Sci Tech 2015 The role of Zirconium in microalloyed steels Feb 2015.pdf (march 2020)